PHYSICAL REVIEW D **85,** 014020 (2012)

Next-to-leading logarithmic QCD contribution of the electromagnetic dipole operator to $\bar{B} \to X_s\gamma\gamma$

H. M. Asatrian,[1] C. Greub,[2] A. Kokulu,[2] and A. Yeghiazaryan[1]

[1]*Yerevan Physics Institute, 0036 Yerevan, Armenia*

[2]*Albert Einstein Center for Fundamental Physics, Institute for Theoretical Physics, University of Bern, CH-3012 Bern, Switzerland*

(Received 13 October 2011; published 18 January 2012)

We calculate the set of $O(\alpha_s)$ corrections to the double differential decay width $d\Gamma_{77}/(ds_1 ds_2)$ for the process $\bar{B} \to X_s\gamma\gamma$ originating from diagrams involving the electromagnetic dipole operator $\mathcal{O}_7$. The kinematical variables s_1 and s_2 are defined as $s_i = (p_b - q_i)^2/m_b^2$, where p_b, q_1, and q_2 are the momenta of the b quark and two photons. While the (renormalized) virtual corrections are worked exactly for a certain range of s_1 and s_2, we retain in the gluon bremsstrahlung process only the leading power with respect to the (normalized) hadronic mass $s_3 = (p_b - q_1 - q_2)^2/m_b^2$ in the underlying triple differential decay width $d\Gamma_{77}/(ds_1 ds_2 ds_3)$. The double differential decay width, based on this approximation, is free of infrared and collinear singularities when combining virtual and bremsstrahlung corrections. The corresponding results are obtained analytically. When retaining all powers in s_3, the sum of virtual and bremsstrahlung corrections contains uncanceled $1/\epsilon$ singularities (which are due to collinear photon emission from the s quark), and other concepts, which go beyond perturbation theory, such as parton fragmentation functions of a quark or a gluon into a photon, are needed which is beyond the scope of our paper.

DOI: 10.1103/PhysRevD.85.014020 PACS numbers: 13.20.He

I. INTRODUCTION

Inclusive rare B-meson decays are known to be a unique source of indirect information about physics at scales of several hundred GeV. In the standard model (SM) all these processes proceed through loop diagrams and thus are relatively suppressed. In the extensions of the SM the contributions stemming from the diagrams with ''new'' particles in the loops can be comparable or even larger than the contribution from the SM. Thus getting experimental information on rare decays puts strong constraints on the extensions of the SM or can even lead to a disagreement with the SM predictions, providing evidence for some ''new physics.''

To make a rigorous comparison between experiment and theory, precise SM calculations for the (differential) decay rates are mandatory. While the branching ratios for $\bar{B} \to X_s\gamma$ [1] and $\bar{B} \to X_s\ell^+\ell^-$ are known today even to next-to-next-to-leading logarithmic (NNLL) precision (for reviews, see [2,3]), other branching ratios, such as the one for $\bar{B} \to X_s\gamma\gamma$ discussed in this paper, are only known to leading logarithmic (LL) precision in the SM [4–7]. In contrast to $\bar{B} \to X_s\gamma$, the current-current operator $\mathcal{O}_2$ has a nonvanishing matrix element for $b \to s\gamma\gamma$ at order α_s^0 precision, leading to an interesting interference pattern with the contributions associated with the electromagnetic dipole operator $\mathcal{O}_7$ already at LL precision. As a consequence, potential new physics should be clearly visible not only in the total branching ratio, but also in the differential distributions.

As the process $\bar{B} \to X_s\gamma\gamma$ is expected to be measured at the planned super B factories in Japan and Italy, it is necessary to calculate the differential distributions to next-to-leading logarithmic (NLL) precision in the SM, in order to fully exploit its potential concerning new physics. The starting point of our calculation is the effective Hamiltonian, obtained by integrating out the heavy particles in the SM, leading to

$$\mathcal{H}_{\text{eff}} = -\frac{4G_F}{\sqrt{2}} V_{ts}^* V_{tb} \sum_{i=1}^{8} C_i(\mu)\mathcal{O}_i(\mu), \tag{1.1}$$

where we use the operator basis introduced in [8]:

$$\begin{aligned}
\mathcal{O}_1 &= (\bar{s}_L\gamma_\mu T^a c_L)(\bar{c}_L\gamma^\mu T_a b_L),\\
\mathcal{O}_2 &= (\bar{s}_L\gamma_\mu c_L)(\bar{c}_L\gamma^\mu b_L),\\
\mathcal{O}_3 &= (\bar{s}_L\gamma_\mu b_L)\sum_q(\bar{q}\gamma^\mu q),\\
\mathcal{O}_4 &= (\bar{s}_L\gamma_\mu T^a b_L)\sum_q(\bar{q}\gamma^\mu T_a q),\\
\mathcal{O}_5 &= (\bar{s}_L\gamma_\mu\gamma_\nu\gamma_\rho b_L)\sum_q(\bar{q}\gamma^\mu\gamma^\nu\gamma^\rho q),\\
\mathcal{O}_6 &= (\bar{s}_L\gamma_\mu\gamma_\nu\gamma_\rho T^a b_L)\sum_q(\bar{q}\gamma^\mu\gamma^\nu\gamma^\rho T_a q),\\
\mathcal{O}_7 &= \frac{e}{16\pi^2}\bar{m}_b(\mu)(\bar{s}_L\sigma^{\mu\nu} b_R)F_{\mu\nu},\\
\mathcal{O}_8 &= \frac{g_s}{16\pi^2}\bar{m}_b(\mu)(\bar{s}_L\sigma^{\mu\nu} T^a b_R)G^a_{\mu\nu}.
\end{aligned} \tag{1.2}$$

The symbols T^a ($a = 1, 8$) denote the $SU(3)$ color generators: g_s and e, the strong and electromagnetic coupling constants. In Eq. (1.2), $\bar{m}_b(\mu)$ is the running b-quark mass in the $\overline{\text{MS}}$ scheme at the renormalization scale μ. As we

 © 2012 American Physical Society

are not interested in *CP*-violation effects in the present paper, we made use of the approximation $V_{ub}V_{us}^* \ll V_{tb}V_{ts}^*$ when writing Eq. (1.1). Furthermore, we also put $m_s = 0$.

While the Wilson coefficients $C_i(\mu)$ appearing in Eq. (1.1) are known to sufficient precision at the low scale $\mu \sim m_b$ since a long time (see e.g. the reviews [2,3] and references therein), the matrix elements $\langle s\gamma\gamma|\mathcal{O}_i|b\rangle$ and $\langle s\gamma\gamma g|\mathcal{O}_i|b\rangle$, which in a NLL calculation are needed to order g_s^2 and g_s, respectively, are not known yet. To calculate the $(\mathcal{O}_i, \mathcal{O}_j)$-interference contributions for the differential distributions at order α_s is in many respects of similar complexity as the calculation of the photon energy spectrum in $\bar{B} \to X_s\gamma$ at order α_s^2 needed for the NNLL computation. There, the individual interference contributions, which all involve extensive calculations, were published in separate papers, sometimes even by two independent groups (see e.g. [9,10]). It therefore cannot be expected that the NLL results for the differential distributions related to $\bar{B} \to X_s\gamma\gamma$ are given in a single paper. As a first step in this NLL enterprise, we derive in the present paper the $O(\alpha_s)$ corrections to the $(\mathcal{O}_7, \mathcal{O}_7)$-interference contribution to the double differential decay width $d\Gamma/(ds_1 ds_2)$ at the partonic level. The variables s_1 and s_2 are defined as $s_i = (p_b - q_i)^2/m_b^2$, where p_b and q_i denote the four-momenta of the b quark and the two photons, respectively.

At order α_s there are contributions to $d\Gamma_{77}/(ds_1 ds_2)$ with three particles (s quark and two photons) and four particles (s quark, two photons, and a gluon) in the final state. These contributions correspond to specific cuts of the b-quark's self-energy at order $\alpha^2 \times \alpha_s$, involving twice the operator $\mathcal{O}_7$. As there are additional cuts, which contain, for example, only one photon, our observable cannot be obtained using the optical theorem, i.e., by taking the absorptive part of the b-quark self-energy at three-loop. We therefore calculate the mentioned contributions with three and four particles in the final state individually.

As discussed in Sec. II, we work out the QCD corrections to the double differential decay width in the kinematical range

$$0 < s_1 < 1, \qquad 0 < s_2 < 1 - s_1.$$

Concerning the virtual corrections, all singularities (after ultraviolet renormalization) are due to soft gluon exchanges and/or collinear gluon exchanges involving the s quark. Concerning the bremsstrahlung corrections (restricted to the same range of s_1 and s_2), there are in addition kinematical situations where collinear photons are emitted from the s quark. The corresponding singularities are not canceled when combined with the virtual corrections, as discussed in detail in Sec. IV. We found, however, that there are no singularities associated with collinear photon emission in the double differential decay width when only retaining the leading power with respect to the (normalized) hadronic mass $s_3 = (p_b - q_1 - q_2)^2/m_b^2$ in the underlying triple differential distribution $d\Gamma_{77}/(ds_1 ds_2 ds_3)$. Our results of this paper are obtained within this "approximation." When going beyond, other concepts which go beyond perturbation theory, such as parton fragmentation functions of a quark or a gluon into a photon, are needed [11].

Before moving to the detailed organization of our paper, we should mention that the inclusive double radiative process $\bar{B} \to X_s\gamma\gamma$ has also been explored in several extensions of the SM [5,7,12]. Also the corresponding exclusive modes, $B_s \to \gamma\gamma$ and $B \to K\gamma\gamma$, have been examined before, both in the SM [6,13–21] and in its extensions [12,17,18,22–30]. We should add that the long-distance resonant effects were also discussed in the literature (see e.g. [6] and references therein). Finally, the effects of photon emission from the spectator quark in the B meson were discussed in [13,17,31].

The remainder of this paper is organized as follows. In Sec. II we work out the double differential distribution $d\Gamma_{77}/(ds_1 ds_2)$ in leading order, i.e., without taking into account QCD corrections to the matrix element $\langle s\gamma\gamma|\mathcal{O}_7|b\rangle$. We retain, however, terms up to order ϵ^1, with ϵ being the dimensional regulator ($d = 4 - 2\epsilon$). Section III is devoted to the calculation of the virtual corrections of order α_s to the double differential decay width. In Sec. IV the corresponding gluon bremsstrahlung corrections to the double differential width are worked out in the approximation where only the leading power with respect to the (normalized) hadronic mass s_3 is retained at the level of the triple differential decay width $d\Gamma_{77}/(ds_1 ds_2 ds_3)$. In Sec. V virtual and bremsstrahlung corrections are combined and the result for the double differential decay width, which is free of infrared and collinear singularities, is given in analytic form. In Sec. VI we illustrate the numerical impact of the NLL corrections and in Sec. VII we present the technical details of our calculations. The paper ends with a short summary in Sec. VIII.

II. LEADING-ORDER RESULT

In this section we discuss the double differential decay width $d\Gamma_{77}/(ds_1 ds_2)$ at lowest order in QCD, i.e. α_s^0. The dimensionless variables s_1 and s_2 are defined everywhere in this paper as

$$s_1 = \frac{(p_b - q_1)^2}{m_b^2}, \qquad s_2 = \frac{(p_b - q_2)^2}{m_b^2}. \tag{2.1}$$

At lowest order the double differential decay width is based on the diagrams shown in Fig. 1. The variables s_1 and s_2 form a complete set of kinematically independent variables for the three-body decay $b \to s\gamma\gamma$. Their kinematical range is as follows:

$$0 \le s_1 \le 1, \qquad 0 \le s_2 \le 1 - s_1.$$

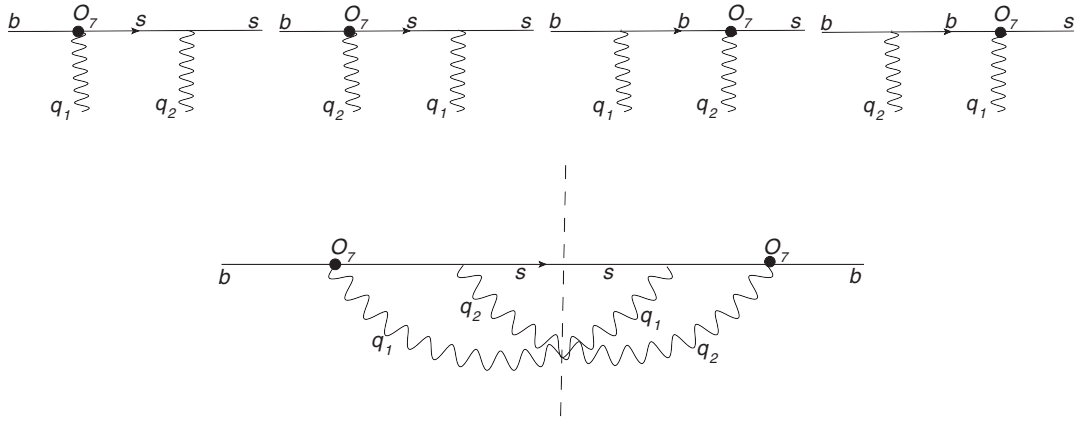

FIG. 1. On the first line the diagrams defining the tree-level amplitude for $b \to s\gamma\gamma$ associated with $\mathcal{O}_7$ are shown. The four-momenta of the b quark, the s quarks, and the two photons are denoted by p_b, p_s, q_1, and q_2, respectively. On the second line the contribution to the decay width corresponding to the interference of the first and second diagrams is shown.

The energies E_1 and E_2 in the rest frame of the b quark of the two photons are related to s_1 and s_2 in a simple way: $s_i = 1 - 2E_i/m_b$. As the energies E_i of the photons have to be away from zero in order to be observed, the values of s_1 and s_2 can be considered to be smaller than 1. By additionally requiring s_1 and s_2 to be larger than zero, we exclude collinear photon emission from the s quark, because $2p_sq_1 = (p_s + q_1)^2 = (p_b - q_2)^2 = s_2m_b^2 > 0$ and $2p_sq_2 = (p_s + q_2)^2 = (p_b - q_1)^2 = s_1m_b^2 > 0$. It is also easy to implement a lower cut on the invariant mass squared s of the two photons by observing that $s = (q_1 + q_2)^2 = 1 - s_1 - s_2$. To parametrize all the mentioned conditions in terms of one parameter c (with $c > 0$), one can proceed as suggested in [5]:

$$s_1 \geq c, \qquad s_2 \geq c, \qquad 1 - s_1 - s_2 \geq c. \tag{2.2}$$

Applying such cuts, the relevant phase-space region in the (s_1, s_2) plane is shown by the shaded area in Fig. 2. Our aim in this paper is to work out the double differential decay width in this restricted area of the s_1 and the s_2 variable also when discussing the gluon bremsstrahlung corrections.[1] In this restricted region of the phase space, the tree-level amplitude is free of infrared and collinear singularities. To exhibit the singularity structure of the virtual corrections discussed in the next section in a transparent way, it is useful to give the leading-order spectrum in $d = 4 - 2\epsilon$ dimensions. We obtain

$$\frac{d\Gamma_{77}^{(0,d)}}{ds_1 ds_2} = \frac{\alpha^2 \bar{m}_b^2(\mu) m_b^3 |C_{7,\mathrm{eff}}(\mu)|^2 G_F^2 |V_{tb}V_{ts}^*|^2 Q_d^2}{1024\pi^5} \left(\frac{\mu}{m_b}\right)^{4\epsilon} r \tag{2.3}$$

with

$$r = \frac{[r_0 + \epsilon(r_1 + r_2 + r_3 + r_4)](1 - s_1 - s_2)}{(1 - s_1)^2 s_1 (1 - s_2)^2 s_2}. \tag{2.4}$$

In r we retained terms of order ϵ^1, while discarding terms of higher order. The individual pieces $r_0, \ldots, r_4$ read

$$\begin{aligned} r_0 = {} & -48s_2^3s_1^3 + 96s_2^2s_1^3 - 56s_2s_1^3 + 8s_1^3 + 96s_2^3s_1^2 \\ & - 192s_2^2s_1^2 + 112s_2s_1^2 - 56s_2^3s_1 + 112s_2^2s_1 - 96s_2s_1 \\ & + 8s_1 + 8s_2^3 + 8s_2, \end{aligned}$$

$$\begin{aligned} r_1 = {} & -16s_2^2s_1^3 + 16s_2s_1^3 - 16s_2^3s_1^2 + 48s_2^2s_1^2 - 32s_2s_1^2 \\ & + 16s_1^2 + 16s_2^3s_1 - 32s_2^2s_1 - 16s_2s_1 + 16s_2^2, \end{aligned}$$

$$\begin{aligned} r_2 = {} & (48s_2^3s_1^3 - 96s_2^2s_1^3 + 56s_2s_1^3 - 8s_1^3 - 96s_2^3s_1^2 \\ & + 192s_2^2s_1^2 - 112s_2s_1^2 + 56s_2^3s_1 - 112s_2^2s_1 + 96s_2s_1 \\ & - 8s_1 - 8s_2^3 - 8s_2)\log(s_1), \end{aligned}$$

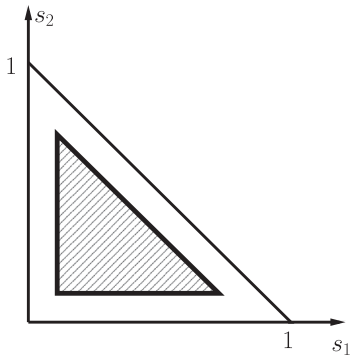

FIG. 2. The relevant phase-space region for (s_1, s_2) used in this paper is shown by the shaded area.

[1] In this case, the normalized invariant mass squared s of the two photons reads $s = 1 - s_1 - s_2 + s_3$, where s_3 is the normalized hadronic mass squared. The condition $1 - s_1 - s_2 \geq c$ then still eliminates two-photon configurations with small invariant mass.

$$r_3 = r_2(s_1 \leftrightarrow s_2),$$

$$\begin{aligned} r_4 = [&48s_2^3s_1^3 - 96s_2^2s_1^3 + 56s_2s_1^3 - 8s_1^3 - 96s_2^3s_1^2 \\ &+ 192s_2^2s_1^2 - 112s_2s_1^2 + 56s_2^3s_1 - 112s_2^2s_1 + 96s_2s_1 \\ &- 8s_1 - 8s_2^3 - 8s_2]\log(1 - s_1 - s_2). \end{aligned}$$

In Eq. (2.3) the symbols $\bar{m}_b(\mu)$ and m_b denote the mass of the b quark in the $\overline{\text{MS}}$ scheme and in the on-shell scheme, respectively.

In $d = 4$ dimensions, the leading-order spectrum (in our restricted phase space) is obtained by simply putting ϵ to zero, obtaining

$$\begin{aligned} \frac{d\Gamma_{77}^{(0)}}{ds_1 ds_2} &= \frac{\alpha^2 \bar{m}_b^2(\mu) m_b^3 |C_{7,\text{eff}}(\mu)|^2 G_F^2 |V_{tb}V_{ts}^*|^2 Q_d^2}{1024\pi^5} \\ &\times \frac{(1 - s_1 - s_2)}{(1 - s_1)^2 s_1 (1 - s_2)^2 s_2} r_0. \end{aligned} \tag{2.5}$$

III. VIRTUAL CORRECTIONS

We now turn to the calculation of the virtual QCD corrections, i.e. to the contributions of order α_s with three particles in the final state. The diagrams defining the (unrenormalized) virtual corrections at the amplitude level are shown on the first four lines of Fig. 3. As the diagrams with a self-energy insertion on the external b- and s-quark legs are taken into account in the renormalization process, these

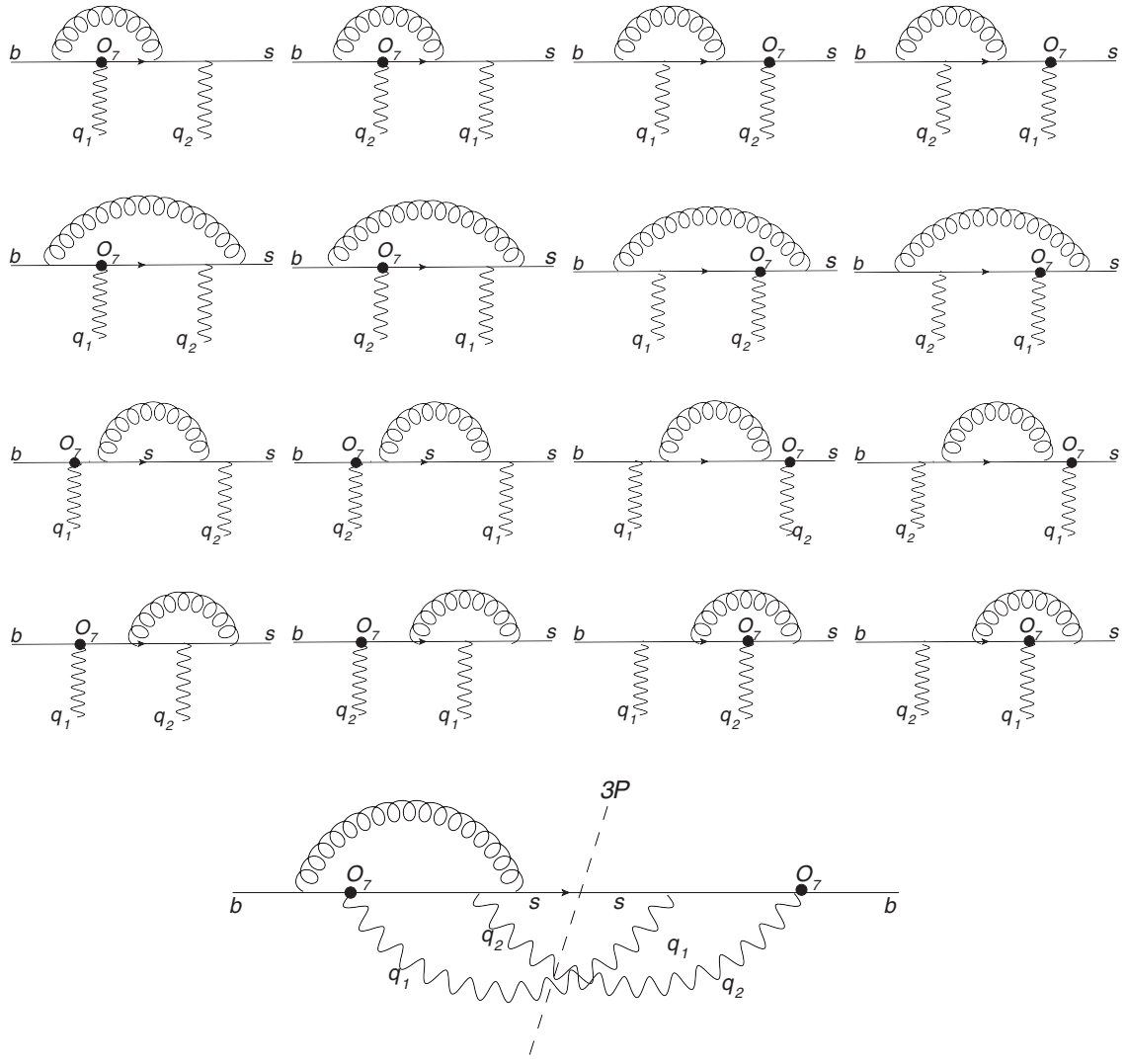

FIG. 3. On the first four lines the diagrams defining the one-loop amplitude for $b \to s\gamma\gamma$ associated with $\mathcal{O}_7$ are shown. Diagrams with self-energy insertions on the external quark legs are not shown. On the last line the contribution to the decay width corresponding to the interference of the first diagram on the second line with the second (tree-level) diagram in Fig. 1 is shown.

diagrams are not shown in Fig. 3. In order to get the (unrenormalized) virtual corrections $d\Gamma_{77}^{\rm bare}/(ds_1 ds_2)$ of order α_s to the decay width, we have to work out the interference of the diagrams on the first four lines in Fig. 3 with the leading-order diagrams in Fig. 1. One of these interference contributions is shown on the last line in Fig. 3. To illustrate the calculational procedure for getting the virtual corrections to the decay width, we describe in Sec. VII A the relevant steps for the particular interference shown in Fig. 3.

In addition, we have to work out the counterterm contributions to the decay width. They can be split into two parts, according to

$$\frac{d\Gamma_{77}^{\rm ct}}{ds_1 ds_2} = \frac{d\Gamma_{77}^{{\rm ct},(A)}}{ds_1 ds_2} + \frac{d\Gamma_{77}^{{\rm ct},(B)}}{ds_1 ds_2}. \tag{3.1}$$

Part (A) involves the Lehmann-Symanzik-Zimmermann factors $\sqrt{Z_{2b}^{\rm OS}}$ and $\sqrt{Z_{2s}^{\rm OS}}$ for the b- and s-quark fields, as well as the self-renormalization constant $Z_{77}^{\overline{\rm MS}}$ of the operator $\mathcal{O}_7$ and $Z_{m_b}^{\overline{\rm MS}}$ renormalizing the factor $\bar{m}_b(\mu)$ present in the operator $\mathcal{O}_7$. The explicit results for these Z factors are given to relevant precision in Appendix C. For part (A) we get

$$\frac{d\Gamma_{77}^{{\rm ct},(A)}}{ds_1 ds_2} = [\delta Z_{2b}^{\rm OS} + \delta Z_{2s}^{\rm OS} + 2\delta Z_{m_b}^{\overline{\rm MS}} + 2\delta Z_{77}^{\overline{\rm MS}}]\frac{d\Gamma_{77}^{(0,d)}}{ds_1 ds_2}, \tag{3.2}$$

where $d\Gamma_{77}^{(0,d)}/(ds_1 ds_2)$ is the leading-order double differential decay width in d dimensions, as given in Eq. (2.3).

The counterterms defining part (B) are due to the insertion of $-i\delta m_b \bar{b}b$ in the internal b-quark line in the leading-order diagrams as indicated in Fig. 4, where

$$\delta m_b = (Z_{m_b}^{\rm OS} - 1)m_b.$$

More precisely, part (B) consists of the interference of the diagrams in Fig. 4 with the leading-order diagrams in Fig. 1.

By adding $d\Gamma_{77}^{\rm bare}/(ds_1 ds_2)$ and $d\Gamma_{77}^{\rm ct}/(ds_1 ds_2)$, we get the result for the renormalized virtual corrections to the spectrum, $d\Gamma_{77}^{(1),{\rm virt}}/(ds_1 ds_2)$. It is useful to decompose this result into two pieces,

$$\frac{d\Gamma_{77}^{(1),{\rm virt}}}{ds_1 ds_2} = \frac{d\Gamma_{77}^{(1,a),{\rm virt}}}{ds_1 ds_2} + \frac{d\Gamma_{77}^{(1,b),{\rm virt}}}{ds_1 ds_2}. \tag{3.3}$$

The infrared and collinear singularities are completely contained in $d\Gamma_{77}^{(1,a),{\rm virt}}/(ds_1 ds_2)$. Explicitly, we obtain

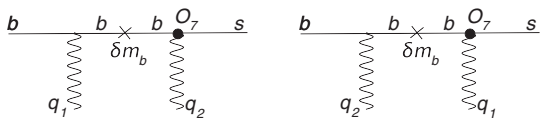

FIG. 4. Counterterm diagrams with a δm_b insertion; see text.

$$\frac{d\Gamma_{77}^{(1,a),{\rm virt}}}{ds_1 ds_2} = \frac{\alpha_s}{4\pi} C_F \left(-\frac{2}{\epsilon^2} + \frac{4\log(s_1+s_2)-5}{\epsilon}\right) \times \left(\frac{\mu}{m_b}\right)^{2\epsilon} \frac{d\Gamma_{77}^{(0,d)}}{ds_1 ds_2}, \tag{3.4}$$

where $d\Gamma_{77}^{(0,d)}/(ds_1 ds_2)$ is understood to be taken exactly as given in Eqs. (2.3) and (2.4), i.e., by including the terms of order ϵ^1 in r. From the explicit expression $d\Gamma_{77}^{(1,a),{\rm virt}}/(ds_1 ds_2)$ we see that the singularity structure consists of a simple singular factor multiplying the corresponding tree-level decay width in d dimensions. We stress that singularities (represented by $1/\epsilon^2$ and $1/\epsilon$ poles) are entirely due to soft and/or collinear gluon exchange. The infrared finite piece $d\Gamma_{77}^{(1,b),{\rm virt}}/(ds_1 ds_2)$ can be written as

$$\frac{d\Gamma_{77}^{(1,b),{\rm virt}}}{ds_1 ds_2} = \frac{\alpha^2 \bar{m}_b^2(\mu) m_b^3 |C_{7,{\rm eff}}(\mu)|^2 G_F^2 |V_{tb}V_{ts}^*|^2 Q_d^2}{1024\pi^5} \times \frac{\alpha_s}{4\pi} C_F \left(\frac{-4r_0(1-s_1-s_2)}{(1-s_1)^2 s_1 (1-s_2)^2 s_2}\log\frac{\mu}{m_b} + \frac{\sum_{i=1}^{20} v_i}{3(1-s_1)^3 s_1 (1-s_2)^3 s_2}\right), \tag{3.5}$$

where the individual quantites $v_1, \ldots, v_{20}$ are relegated to Appendix A.

IV. BREMSSTRAHLUNG CORRECTIONS

We now turn to the calculation of the bremsstrahlung QCD corrections, i.e. to the contributions of order α_s with four particles in the final state. Before going into detail, we mention that the kinematical range of the variables s_1 and s_2 defined in Eq. (2.1) is given in this case by $0 \le s_1 \le 1$ and $0 \le s_2 \le 1$. Nevertheless, we consider in this paper only the range which is also accessible to the three-body decay $b \to s\gamma\gamma$, i.e., $0 \le s_1 \le 1$ and $0 \le s_2 \le 1 - s_1$ or, more precisely, by its restricted version specified in Eq. (2.2).

The diagrams defining the bremsstrahlung corrections at the amplitude level are shown in the first line of Fig. 5. The amplitude squared, needed to get the (double differential) decay width, can be written as a sum of interferences of the different diagrams on the first line in Fig. 5. One such interference is shown on the second line of the same figure. The four particle final state is described by five independent kinematical variables. In the first attempt we worked out the decay width by keeping s_1 and s_2 differential and integrating over the three remaining variables. Proceeding in this way, we found that the infrared and collinear singularities in the bremsstrahlung spectrum do not cancel when adding the virtual corrections. The sum still contains $1/\epsilon$ poles, but no $1/\epsilon^2$ poles. While, as already mentioned in Sec. III, the only sources of the singularities in the virtual corrections in our restricted range of s_1 and s_2 are due to soft gluon emission and/or collinear emission of

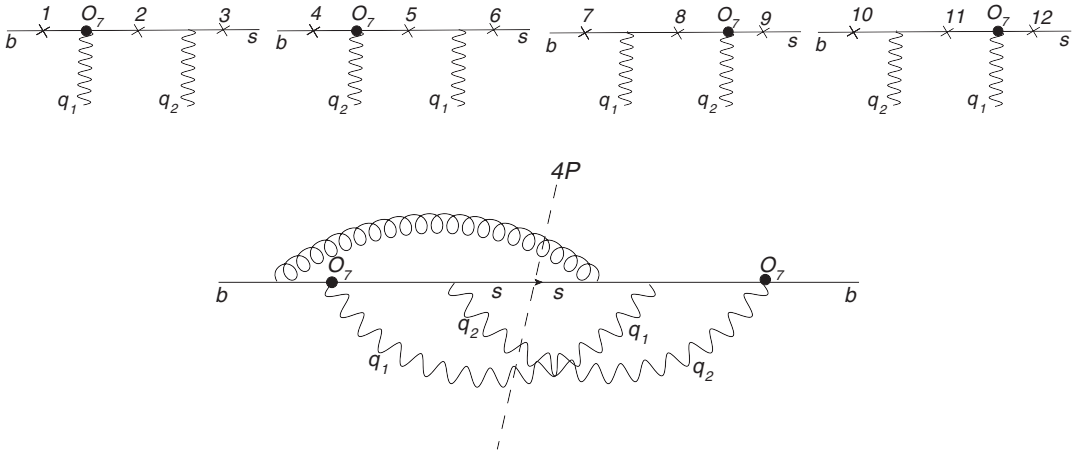

FIG. 5. On the first line the diagrams defining the gluon bremsstrahlung corrections to $b \to s\gamma\gamma$ are shown at the amplitude level. The crosses in the graphs stand for the possible emission places of the gluon. On the second line the contribution to the decay width corresponding to the interference of diagram 1 with diagram 6 is illustrated.

gluons from the s quark; we found after analyzing the bremsstrahlung kinematics more carefully that there are situations where one of the photons can become collinear with the s quark. This is the reason why there is no cancellation of singularities when combining virtual and bremsstrahlung corrections. Realizing that for (formally) zero hadronic mass of the (s, g) system collinear photon emission is kinematically impossible led us to the idea that we should first look at the triple differential decay width $d\Gamma_{77}/(ds_1 ds_2 ds_3)$, where $s_3 = (p_s + p_g)^2/m_b^2$ is the normalized hadronic mass squared. Our conjecture was that the double differential decay width, based on the triple differential decay width in which only the leading power terms with respect to s_3 are retained, should lead to a finite result when combined with the virtual corrections.

We therefore worked out the leading power of this quantity with respect to s_3, denoting it by $d\Gamma_{77}^{\text{leading power}}/(ds_1 ds_2 ds_3)$. The leading power, which is of order $1/s_3$ (modified by epsilontic dimensional regulators), is supposed to be a good approximation for low values of the hadronic mass. An approximation to the double differential decay width $d\Gamma_{77}^{(1),\text{brems}}/(ds_1 ds_2)$ due to gluon bremsstrahlung corrections is then obtained by integrating $d\Gamma_{77}^{\text{leading power}}/(ds_1 ds_2 ds_3)$ over s_3, which runs in the range $s_3 \in [0, s_1 \cdot s_2]$. The approximation is obviously accurate for small values of $s_1 \cdot s_2$. As $s_1 \cdot s_2$ is at most $1/4$, the approximation is expected not to be bad in the full region of s_1 and s_2 considered in this paper. The technical details of the calculation of the leading power with respect to s_3 in the triple differential decay width are illustrated in Sec. VII B for the interference of diagram 1 with diagram 6, as shown in the second line of Fig. 5.

Indeed, we find that the infrared and collinear singularities cancel when combining the approximated version of $d\Gamma_{77}^{(1),\text{brems}}/(ds_1 ds_2)$ with the virtual corrections $d\Gamma_{77}^{(1),\text{virt}}/(ds_1 ds_2)$.

When going beyond this approximation other concepts, which go beyond perturbation theory, such as parton fragmentation functions of a quark or a gluon into a photon, are needed [11]. We do not address this issue in this paper.

The result of combined virtual and bremsstrahlung corrections is explicitly presented in the next section.

V. FINAL RESULT FOR THE DECAY WIDTH AT ORDER α_s

The complete order α_s correction to the double differential decay width $d\Gamma_{77}/(ds_1 ds_2)$ is obtained by adding the renormalized virtual corrections from Sec. III and the bremsstrahlung corrections discussed in Sec. IV. Explicitly we get

$$\frac{d\Gamma_{77}^{(1)}}{ds_1 ds_2} = \frac{\alpha^2 \bar{m}_b^2(\mu) m_b^3 |C_{7,\text{eff}}(\mu)|^2 G_F^2 |V_{tb} V_{ts}^*|^2 Q_d^2}{1024\pi^5} \times \frac{\alpha_s}{4\pi} C_F \left[\frac{-4r_0(1 - s_1 - s_2)}{(1 - s_1)^2 s_1 (1 - s_2)^2 s_2} \log\frac{\mu}{m_b} + f \right], \tag{5.1}$$

where f is decomposed as

$$f = \frac{(1 - s_1 - s_2)(f_1 + f_2 + f_3 + f_4 + f_5 + f_6 + f_7 + f_8 + f_9 + f_{15} + f_{16} + f_{17})}{3(1 - s_1)^3 s_1 (1 - s_2)^3 s_2} + \frac{f_{10} + f_{11} + f_{12} + f_{13} + f_{14}}{3(1 - s_1)^3 s_1 (1 - s_2)^3 s_2}. \tag{5.2}$$

The individual quantities $f_1, \ldots, f_{17}$ read

$$\begin{aligned}
f_1 = {} & -16\pi^2 s_2^3 s_1^5 - 16\pi^2 s_2^5 s_1^3 + 48\pi^2 s_2^2 s_1^5 + 48\pi^2 s_2^5 s_1^2 - 48\pi^2 s_2 s_1^5 - 48\pi^2 s_2^5 s_1 + 16\pi^2 s_1^5 + 16\pi^2 s_2^5 - 168 s_1^3 - 168 s_2^3 \\
& + (1104 + 160\pi^2) s_2^4 s_1^4 + (-3360 - 400\pi^2) s_2^3 s_1^4 + (3432 + 304\pi^2) s_2^2 s_1^4 + (-1296 - 64\pi^2) s_2 s_1^4 + (120 - 16\pi^2) s_1^4 \\
& + (-3360 - 400\pi^2) s_2^4 s_1^3 + (10416 + 1152\pi^2) s_2^3 s_1^3 + (-10872 - 1056\pi^2) s_2^2 s_1^3 + (3984 + 368\pi^2) s_2 s_1^3 \\
& + (3432 + 304\pi^2) s_2^4 s_1^2 + (-10872 - 1056\pi^2) s_2^3 s_1^2 + (12096 + 1088\pi^2) s_2^2 s_1^2 + (-4872 - 448\pi^2) s_2 s_1^2 \\
& + (216 + 16\pi^2) s_1^2 + (-1296 - 64\pi^2) s_2^4 s_1 + (3984 + 368\pi^2) s_2^3 s_1 + (-4872 - 448\pi^2) s_2^2 s_1 \\
& + (2352 + 224\pi^2) s_2 s_1 + (-168 - 16\pi^2) s_1 + (120 - 16\pi^2) s_2^4 + (216 + 16\pi^2) s_2^2 + (-168 - 16\pi^2) s_2,
\end{aligned}$$

$$f_2 = 48 s_2 (1 - s_1)(1 - s_2)^2 (6 s_2 s_1^3 - 6 s_1^3 - 11 s_2 s_1^2 + 15 s_1^2 + 3 s_2 s_1 - 9 s_1 + 2) \log(1 - s_1),$$

$$\begin{aligned}
f_3 = {} & 24(1 - s_1)(1 - s_2)(30 s_2^3 s_1^3 - 64 s_2^2 s_1^3 + 41 s_2 s_1^3 - 7 s_1^3 - 60 s_2^3 s_1^2 + 128 s_2^2 s_1^2 \\
& - 82 s_2 s_1^2 + 37 s_2^3 s_1 - 78 s_2^2 s_1 + 76 s_2 s_1 - 7 s_1 - 7 s_2^3 - 7 s_2) \log(s_1),
\end{aligned}$$

$$\begin{aligned}
f_4 = {} & -48(1 - s_1)(1 - s_2)(s_2^2 s_1^4 - s_2 s_1^4 - 5 s_2^3 s_1^3 + 9 s_2^2 s_1^3 - 5 s_2 s_1^3 + s_1^3 + 9 s_2^3 s_1^2 \\
& - 20 s_2^2 s_1^2 + 13 s_2 s_1^2 - 5 s_2^3 s_1 + 12 s_2^2 s_1 - 12 s_2 s_1 + s_1 + s_2^3 + s_2) \log^2(s_1),
\end{aligned}$$

$$\begin{aligned}
f_7 = {} & 96(1 - s_1)(1 - s_2)(6 s_2^3 s_1^3 - 12 s_2^2 s_1^3 + 7 s_2 s_1^3 - s_1^3 - 12 s_2^3 s_1^2 + 24 s_2^2 s_1^2 - 14 s_2 s_1^2 + 7 s_2^3 s_1 \\
& - 14 s_2^2 s_1 + 12 s_2 s_1 - s_1 - s_2^3 - s_2) \log(s_1) \log(s_2),
\end{aligned}$$

$$\begin{aligned}
f_9 = {} & -96(1 - s_1)(1 - s_2)(6 s_2^3 s_1^3 - 12 s_2^2 s_1^3 + 7 s_2 s_1^3 - s_1^3 - 12 s_2^3 s_1^2 + 24 s_2^2 s_1^2 - 14 s_2 s_1^2 \\
& + 7 s_2^3 s_1 - 14 s_2^2 s_1 + 12 s_2 s_1 - s_1 - s_2^3 - s_2) \log(s_1 + s_2),
\end{aligned}$$

$$\begin{aligned}
f_{10} = {} & 96(1 - s_1)(1 - s_2)^2 (s_2 s_1^5 - s_1^5 + 2 s_2^2 s_1^4 - 5 s_2 s_1^4 + 3 s_1^4 + s_2^3 s_1^3 - 5 s_2^2 s_1^3 + 8 s_2 s_1^3 \\
& - 2 s_1^3 - s_2^3 s_1^2 + 4 s_2^2 s_1^2 - 4 s_2 s_1^2 + s_1^2 - 4 s_2^2 s_1 + 3 s_2 s_1 - s_1 - s_2^2 + s_2) \log(1 - s_1) \log(s_1 + s_2),
\end{aligned}$$

$$\begin{aligned}
f_{11} = {} & -96(1 - s_1)(1 - s_2)(s_2^2 s_1^5 - s_2 s_1^5 - 10 s_2^3 s_1^4 + 19 s_2^2 s_1^4 - 11 s_2 s_1^4 + 2 s_1^4 - 11 s_2^4 s_1^3 + 53 s_2^3 s_1^3 - 77 s_2^2 s_1^3 + 41 s_2 s_1^3 \\
& - 2 s_1^3 + 21 s_2^4 s_1^2 - 76 s_2^3 s_1^2 + 94 s_2^2 s_1^2 - 49 s_2 s_1^2 + 2 s_1^2 - 11 s_2^4 s_1 + 38 s_2^3 s_1 - 46 s_2^2 s_1 \\
& + 25 s_2 s_1 - 2 s_1 + s_2^4 - s_2^3 + s_2^2 - s_2) \log(s_1) \log(s_1 + s_2),
\end{aligned}$$

$$\begin{aligned}
f_{14} = {} & 48(1 - s_1)(1 - s_2)(s_2^2 s_1^5 - s_2 s_1^5 - 21 s_2^3 s_1^4 + 40 s_2^2 s_1^4 - 22 s_2 s_1^4 + 3 s_1^4 - 21 s_2^4 s_1^3 + 106 s_2^3 s_1^3 - 153 s_2^2 s_1^3 + 79 s_2 s_1^3 \\
& - 3 s_1^3 + s_2^5 s_1^2 + 40 s_2^4 s_1^2 - 153 s_2^3 s_1^2 + 188 s_2^2 s_1^2 - 95 s_2 s_1^2 + 3 s_1^2 - s_2^5 s_1 - 22 s_2^4 s_1 + 79 s_2^3 s_1 - 95 s_2^2 s_1 + 50 s_2 s_1 \\
& - 3 s_1 + 3 s_2^4 - 3 s_2^3 + 3 s_2^2 - 3 s_2) \log^2(s_1 + s_2),
\end{aligned}$$

$$\begin{aligned}
f_{15} = {} & 96 s_1 (1 - s_2)^2 (s_2 s_1^4 - s_1^4 + s_2^2 s_1^3 - 4 s_2 s_1^3 + 3 s_1^3 - 5 s_2^2 s_1^2 + 8 s_2 s_1^2 - 2 s_1^2 \\
& + 7 s_2^2 s_1 - 11 s_2 s_1 + s_1 - 2 s_2^2 + 5 s_2 - 1) \mathrm{Li}_2(s_1),
\end{aligned}$$

$$\begin{aligned}
f_{16} = {} & 96(1 - s_1)(1 - s_2)(s_2^2 s_1^4 - 2 s_2 s_1^4 + s_1^4 + 8 s_2^3 s_1^3 - 17 s_2^2 s_1^3 + 12 s_2 s_1^3 - 3 s_1^3 + s_2^4 s_1^2 - 17 s_2^3 s_1^2 + 32 s_2^2 s_1^2 - 20 s_2 s_1^2 \\
& - 2 s_2^4 s_1 + 12 s_2^3 s_1 - 20 s_2^2 s_1 + 20 s_2 s_1 - 2 s_1 + s_2^4 - 3 s_2^3 - 2 s_2) \mathrm{Li}_2(1 - s_1 - s_2),
\end{aligned}$$

$$\begin{aligned}
& f_5 = f_2(s_1 \leftrightarrow s_2), \qquad f_6 = f_3(s_1 \leftrightarrow s_2), \qquad f_8 = f_4(s_1 \leftrightarrow s_2), \\
& f_{12} = f_{10}(s_1 \leftrightarrow s_2), \qquad f_{13} = f_{11}(s_1 \leftrightarrow s_2), \qquad f_{17} = f_{15}(s_1 \leftrightarrow s_2).
\end{aligned}$$

The order α_s correction $d\Gamma_{77}^{(1)}/(ds_1 ds_2)$ in Eq. (5.1) to the double differential decay width for $b \to X_s \gamma\gamma$ is the main result of our paper.

TABLE I. Values of the relevant input parameters

Parameter	Value
m_b	4.8 GeV
m_t	175 GeV
m_W	80.4 GeV
m_Z	91.19 GeV
G_F	$1.166\,37 \times 10^{-5}$ GeV^{-2}
$V_{tb}V_{ts}^*$	0.04
α^{-1}	137
$\alpha_s(M_Z)$	0.119

VI. SOME NUMERICAL ILLUSTRATIONS

In the previous sections we calculated the virtual and bremsstrahlung QCD corrections which were the missing ingredient in order to obtain the $(\mathcal{O}_7, \mathcal{O}_7)$ contribution to the double differential decay width for $\bar{B} \to X_s\gamma\gamma$ at NLL precision. The Wilson coefficient $C_{7,\text{eff}}(\mu)$ at the low scale $(\mu \sim m_b)$ which is needed up to order α_s, i.e.,

$$C_{7,\text{eff}}(\mu) = C^0_{7,\text{eff}}(\mu) + \frac{\alpha_s(\mu)}{4\pi} C^1_{7,\text{eff}}(\mu), \tag{6.1}$$

has been known for a long time (see Ref. [8] and references therein). Numerical values for the input parameters and for this Wilson coefficient at various values for the scale μ, together with the numerical values of $\alpha_s(\mu)$, are given in Tables I and II, respectively. The NLL prediction reads

TABLE II. $\alpha_s(\mu)$ and the Wilson coefficient $C_{7,\text{eff}}(\mu)$ at different values of the scale μ.

	$\alpha_s(\mu)$	$C^0_{7,\text{eff}}(\mu)$	$C^1_{7,\text{eff}}(\mu)$
$\mu = m_W$	0.1213	−0.1957	−2.3835
$\mu = 2m_b$	0.1818	−0.2796	−0.1788
$\mu = m_b$	0.2175	−0.3142	0.4728
$\mu = m_b/2$	0.2714	−0.3556	1.0794

$$\frac{d\Gamma_{77}}{ds_1 ds_2} = \frac{d\Gamma^{(0)}_{77}}{ds_1 ds_2} + \frac{d\Gamma^{(1)}_{77}}{ds_1 ds_2}, \tag{6.2}$$

where the first and second terms of the right-hand side (rhs) are given in Eqs. (2.5) and (5.1), respectively.

To illustrate our results, we first rewrite the $\overline{\text{MS}}$ mass $\bar{m}_b(\mu)$ in Eq. (6.2) in terms of the pole mass m_b, using the one-loop relation

$$\bar{m}_b(\mu) = m_b\left[1 - \frac{\alpha_s(\mu)}{4\pi}\left(8\log\frac{\mu}{m_b} + \frac{16}{3}\right)\right].$$

We then insert $C_{7,\text{eff}}(\mu)$ in the expanded form (6.1) and expand the resulting expression for $d\Gamma_{77}/(ds_1 ds_2)$ with respect to α_s, discarding terms of order α_s^2. This defines

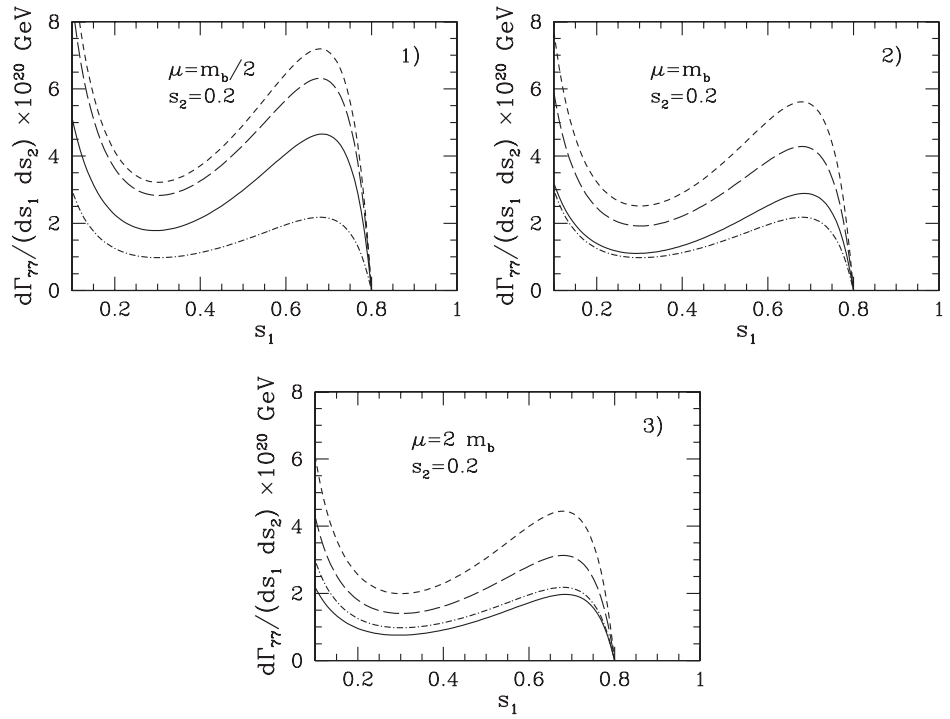

FIG. 6. Double differential decay width $d\Gamma_{77}/(ds_1 ds_2)$ as a function of s_1 for s_2 fixed at $s_2 = 0.2$. The dash-dotted, the short-dashed, and the solid lines show the result when neglecting QCD effects, the LL result, and the NLL result, respectively. The long-dashed lines represent the (partial) NLL result in which the virtual and bremsstrahlung corrections worked out in this paper are switched off (see text for more details). In frames (1), (2), and (3) the renormalization scale is chosen to be $\mu = m_b/2$, $\mu = m_b$, and $\mu = 2m_b$, respectively.

the NLL result. The corresponding LL result is obtained by also discarding the order α_s^1 term. In Fig. 6 the LL and the NLL results are shown by the short-dashed and the solid lines, respectively.

In our procedure the NLL corrections have three sources: (a) α_s corrections to the Wilson coefficient $C_{7,\mathrm{eff}}(\mu)$, (b) expressing $\bar{m}_b(\mu)$ in terms of the pole mass m_b, and (c) virtual- and real-order α_s corrections to the matrix elements. To illustrate the effect of source (c), which is worked out for the first time in this paper, we show in Fig. 6 (by the long-dashed line) the (partial) NLL result in which source (c) is switched off. We conclude that effect (c) is roughly of equal importance as the combined effects of (a) and (b).

For completeness we show in this figure (by the dash-dotted line) also the result when QCD is completely switched off, which amounts to putting $\mu = m_W$ in the LL result.

From Fig. 6 we see that the NLL results are substantially smaller (typically by 50% or slightly more) than those at LL precision, which is also the case when choosing other values for s_2.

In the numerical discussion above, we have systematically converted the running b-quark mass $\bar{m}_b(\mu)$ in terms of the pole mass m_b. As perturbative expansions often behave better when expressed in terms of the running mass, we also studied the results obtained when systematically converting m_b in terms of $\bar{m}_b(\mu)$. After also doing this version, we observe the following: Generally speaking, NLL corrections are not small for both cases, when taking into account the full range of μ, i.e., $m_b/2 < \mu < 2m_b$. More precisely, in the $\overline{\mathrm{MS}}$ version they are large for $\mu = m_b/2$ and smaller for larger values of μ, while in the pole mass version they are large for all values of μ.

We stress that the numerically important contributions involving the operator O_2 are not discussed in our paper. Therefore, the issue concerning the reduction of the μ dependence at NLL precision cannot be addressed at this level. Our main point in this section was to illustrate that the NLL corrections to the process $\bar{B} \to X_s\gamma\gamma$ are expected to be rather large.

VII. TECHNICAL DETAILS ABOUT OUR CALCULATIONS

We first describe the general setup of our calculations and then discuss in Secs. VII A and VII B the calculation of the virtual and the bremsstrahlung corrections for the interference diagrams shown in the last lines of Figs. 3 and 5, respectively.

The starting point is the general expression for the total decay width of the massive b quark with momentum p_b decaying into $3 \le n \le 4$ massless final-state particles with momenta k_i,

$$\begin{aligned}\Gamma_{1\to n} &= \frac{1}{2m_b}\left(\prod_{i=1}^{n}\int\frac{d^{d-1}k_i}{(2\pi)^{d-1}2E_i}\right)(2\pi)^d\delta^{(d)}\left(p_b-\sum_{i=1}^{n}k_i\right)|M_n|^2\\ &= \frac{1}{2m_b}(2\pi)^n\left(\prod_{i=1}^{n-1}\int\frac{d^dk_i}{(2\pi)^d}\delta(k_i^2)\theta(k_i^0)\right)\\ &\quad\times\delta\left(\left(p_b-\sum_{i=1}^{n-1}k_i\right)^2\right)\theta\left(p_b^0-\sum_{i=1}^{n-1}k_i^0\right)|M_n|^2, \qquad (7.1)\end{aligned}$$

where the squared Feynman amplitude $|M_n|^2$ is always understood to be summed over final spin, polarization, and color states, and averaged over the spin directions and colors of the decaying b quark. It also includes a factor of $1/2$ for the two identical particles in the final state, i.e. the photons. Furthermore, $d = 4 - 2\epsilon$ denotes the space-time dimension that we use to regulate the ultraviolet, infrared, and collinear singularities.

The double differential decay rate $d\Gamma_{77}/(ds_1 ds_2)$ is obtained from Eq. (7.1) by multiplying the integrand on the rhs with the delta functions $\delta(s_1 - (p_b - q_1)^2/m_b^2)$ and $\delta(s_2 - (p_b - q_2)^2/m_b^2)$ [32], where p_b and q_1, q_2 denote the four momenta of the b quark and the photons, respectively. For the bremsstrahlung corrections, as mentioned in Sec. IV, we need to consider also the triple differential decay width $d\Gamma_{77}/(ds_1 ds_2 ds_3)$, where $s_3 = (p_b - q_1 - q_2)^2/m_b^2$ is the normalized hadronic mass squared. The triple differential decay width is obtained by multiplying the integrand with the additional delta function $\delta(s_3 - (p_b - q_1 - q_2)^2/m_b^2)$. Finally, the delta functions just mentioned and all of the delta functions present in Eq. (7.1) can be rewritten as differences of propagators as follows [33,34]:

$$\delta(q^2 - m^2) = \frac{1}{2\pi i}\left(\frac{1}{q^2 - m^2 - i0} - \frac{1}{q^2 - m^2 + i0}\right). \qquad (7.2)$$

In this step the phase-space integrations are converted into loop integrations (which can be combined with possible loop integrations already present in $|M_n|^2$). By subsequently doing tensor reductions, the (differential) decay width can be written as a linear combination of scalar integrals. The systematic Laporta algorithm [35], based on integration-by-part techniques first proposed in [36,37], can then be applied to reduce the scalar integrals to a small number of simpler integrals, usually referred to as the master integrals (MIs). For this reduction we used the AIR and FIRE implementations [38,39] of the Laporta algorithm. After the reduction process, it usually happens that some MIs contain propagators which were introduced via (7.2) with zero or negative power. In this case the $\pm i0$ prescription becomes irrelevant and as a consequence these MIs are zero. In the remaining MIs we convert the propagators introduced via (7.2) back to delta functions. Thus, we are left with phase-space MIs (which can contain loop integrations as well). The final task is then to calculate

these MIs, i.e. to perform possible loop integrations together with the phase-space integrations.

Very often we had to deal with MIs which we were not able to evaluate by direct integration of their integral representation in terms of Feynman parameters and/or phase-space parameters. A powerful tool to be used in these cases is the differential equation method [33,34,40,41]. The goal of this method is to employ the output of the reduction procedure for a given topology to build differential equations which are satisfied by the MIs of that topology. In our case, we consider differential equations with respect to s_1 and s_2 and also with respect to s_3 for the case of bremsstrahlung corrections. With these methods we were able to obtain analytic expressions for all master integrals appearing in the calculation of the various diagrams.

A. Details about the calculation of virtual corrections

To illustrate our methods for the virtual corrections, we take as an example the interference diagram shown on the last line of Fig. 3. In this case we have five MIs. Four of them can be solved by means of direct integration on Feynman parameters. To calculate the last one (called P_{1111}), we solve the differential equations with respect to s_1 and s_2 and get the solution which we denote as Q_{1111}. At this level Q_{1111} contains integration constants (which are not fixed by the differential equations). To get the integration constants, we proceed in the following way. Using Feynman parametrization for the loop integral, we write the MI P_{1111} as

$$P_{1111} = s_1^{-\epsilon} s_2^{-\epsilon} (1 - s_1 - s_2)^{-\epsilon} \times \int_0^1 g_0(s_1, s_2, \epsilon, u, v, y) du dv dy, \quad (7.3)$$

where u, v, and y are Feynman parameters (all of them running from 0 to 1). The factor $s_1^{-\epsilon} s_2^{-\epsilon} (1 - s_1 - s_2)^{-\epsilon}$ is coming from the phase space [see Eq. (B2) in Appendix B 1]. One then can put $s_2 = 0$ in $g_0(s_1, s_2, \epsilon, u, v, y)$ and integrate on the Feynman parameters, which defines the new function

$$g_1(s_1, \epsilon) = \int_0^1 g_0(s_1, 0, \epsilon, u, v, y) du dv dy. \quad (7.4)$$

We managed to work out the leading term of the expansion of $g_1(s_1, \epsilon)$ on s_1 around zero, which is proportional to s_1^{-2}. From this, we immediately get the leading term of the expansion of P_{1111} on s_2 and s_1 (which is proportional to s_2^0/s_1^2). Comparing the result of this calculation with the corresponding expansion of the solution Q_{1111} of the differential equations, we could determine all integration constants.

B. Details about the calculation of bremsstrahlung corrections

To illustrate our methods for the bremsstrahlung corrections, we take as an example the interference diagram shown on the last line of Fig. 5. In this case we obtain three MIs, denoted by P_{00}, P_{10}, and P_{11}. Writing the diagram as a linear combination of the MIs, we see that the leading power (with respect to s_3) of all three coefficients (in front of the MIs) is of the order $1/s_3$. Keeping in mind that we are taking into account only terms proportional to the leading power in s_3 at the level of the triple differential decay width (as extensively discussed in Sec. IV), it is sufficient to work out the MIs to zeroth power in s_3, including the epsilontic regulator, i.e., $s_3^{0-n\epsilon}$ (in our case only $n = 1$ and $n = 2$ occur).

The simplest MI, P_{00}, which corresponds to the pure phase space [see Eq. (B4) in Appendix B 2], can be easily solved by means of direct integration. For P_{10} the solution of the differential equation with respect to s_3 can be represented in the limit $s_3 \to 0$ in the form

$$P_{10} = a_1(s_1, s_2, \epsilon) s_3^{-\epsilon} + a_2(s_1, s_2, \epsilon) s_3^{-2\epsilon}, \quad (7.5)$$

where the function $a_1(s_1, s_2, \epsilon)$ is fully determined. To find the function $a_2(s_1, s_2, \epsilon)$, we use differential equations with respect to s_1 and s_2. In this way, we could find $a_2(s_1, s_2, \epsilon)$ up to integration constants. To determine these constants, we managed to calculate the MI for specific values of s_1, s_2, and $s_3 \to 0$. In the same way we also calculated the MI P_{11}.

VIII. SUMMARY

In the present work we calculated the set of the $O(\alpha_s)$ corrections to the decay process $\bar{B} \to X_s \gamma\gamma$ originating from diagrams involving the electromagnetic dipole operator $\mathcal{O}_7$. To perform this calculation it is necessary to work out diagrams with three particles (s quark and two photons) and four particles (s quark, two photons, and a gluon) in the final state. From the technical point of view, the calculation was made possible by the use of the Laporta algorithm to identify the needed master integrals and by applying the differential equation method to solve the master integrals. When calculating the bremsstrahlung corrections, we take into account only terms proportional to the leading power of the hadronic mass. We find that the infrared and collinear singularities cancel when combining the above mentioned approximated version of bremsstrahlung corrections with the virtual corrections. The numerical impact of the NLL corrections is not small: for $d\Gamma_{77}/(ds_1 ds_2)$ the NLL results are approximately 50% smaller than those at LL precision.

ACKNOWLEDGMENTS

C. G. and A. K. were partially supported by the Swiss National Foundation and by the Helmholz Association

through funds provided to the virtual institute "Spin and strong QCD" (VH-VI-231). The Albert Einstein Center for Fundamental Physics (Bern), to which C. G. and A. K. are affiliated, is supported by the "Innovations-und Kooperationsprojekt C-13 of the Schweizerische Universitätskonferenz SUK/CRUS." H. A. and A. Y. were supported by the Armenian State Committee of Science under Contract No. 11-1c014. Finally, we thank A. V. Smirnov for helpful email exchanges concerning his program FIRE [39].

APPENDIX A: EXPLICIT RESULTS FOR THE FUNCTIONS v_i DEFINING THE VIRTUAL CORRECTIONS

The functions v_i appearing in Eq. (3.5) read

$$\begin{aligned}
v_1 = {} & (1-s_1-s_2)(-16\pi^2 s_2^3 s_1^5 - 16\pi^2 s_2^5 s_1^3 + 48\pi^2 s_2^2 s_1^5 + 48\pi^2 s_2^5 s_1^2 - 48\pi^2 s_2 s_1^5 - 48\pi^2 s_2^5 s_1 + 16\pi^2 s_1^5 + 16\pi^2 s_2^5 \\
& + (2112 - 104\pi^2) s_2^4 s_1^4 + (392\pi^2 - 6384) s_2^3 s_1^4 + (6672 - 532\pi^2) s_2^2 s_1^4 + (288\pi^2 - 2736) s_2 s_1^4 + (336 - 60\pi^2) s_1^4 \\
& + (392\pi^2 - 6384) s_2^4 s_1^3 + (19584 - 1224\pi^2) s_2^3 s_1^3 + (1452\pi^2 - 20784) s_2^2 s_1^3 + (7872 - 600\pi^2) s_2 s_1^3 \\
& + (44\pi^2 - 288) s_1^3 + (6672 - 532\pi^2) s_2^4 s_1^2 + (1452\pi^2 - 20784) s_2^3 s_1^2 + (23904 - 1728\pi^2) s_2^2 s_1^2 \\
& + (740\pi^2 - 10128) s_2 s_1^2 + (336 - 28\pi^2) s_1^2 + (288\pi^2 - 2736) s_2^4 s_1 + (7872 - 600\pi^2) s_2^3 s_1 \\
& + (740\pi^2 - 10128) s_2^2 s_1 + (5376 - 392\pi^2) s_2 s_1 + (28\pi^2 - 384) s_1 + (336 - 60\pi^2) s_2^4 \\
& + (44\pi^2 - 288) s_2^3 + (336 - 28\pi^2) s_2^2 + (28\pi^2 - 384) s_2),
\end{aligned}$$

$$\begin{aligned}
v_2 = {} & -96(1-s_1)(1-s_2)(1-s_1-s_2)(3 s_2^3 s_1^3 - 4 s_2^2 s_1^3 + s_2 s_1^3 - 5 s_2^3 s_1^2 + 7 s_2^2 s_1^2 - 2 s_2 s_1^2 \\
& - s_1^2 + 2 s_2^3 s_1 - 3 s_2^2 s_1 + 3 s_2 s_1 - s_2^2) \log(s_1),
\end{aligned}$$

$$\begin{aligned}
v_3 = {} & -24(1-s_1)(1-s_2)(1-s_1-s_2)(2 s_2^2 s_1^4 - 2 s_2 s_1^4 - 4 s_2^3 s_1^3 + 6 s_2^2 s_1^3 - 3 s_2 s_1^3 \\
& + s_1^3 + 6 s_2^3 s_1^2 - 16 s_2^2 s_1^2 + 12 s_2 s_1^2 - 3 s_2^3 s_1 + 10 s_2^2 s_1 - 12 s_2 s_1 + s_1 + s_2^3 + s_2) \log^2(s_1),
\end{aligned}$$

$$\begin{aligned}
v_4 = {} & 48(1-s_1)(1-s_2)(1-s_1-s_2)(6 s_2^3 s_1^3 - 12 s_2^2 s_1^3 + 7 s_2 s_1^3 - s_1^3 - 12 s_2^3 s_1^2 + 24 s_2^2 s_1^2 \\
& - 14 s_2 s_1^2 + 7 s_2^3 s_1 - 14 s_2^2 s_1 + 12 s_2 s_1 - s_1 - s_2^3 - s_2) \log(s_1) \log(s_2),
\end{aligned}$$

$$\begin{aligned}
v_5 = {} & 48(1-s_1)(1-s_2)(1-s_1-s_2)(6 s_2^3 s_1^3 - 12 s_2^2 s_1^3 + 7 s_2 s_1^3 - s_1^3 - 12 s_2^3 s_1^2 + 24 s_2^2 s_1^2 \\
& - 14 s_2 s_1^2 + 7 s_2^3 s_1 - 14 s_2^2 s_1 + 12 s_2 s_1 - s_1 - s_2^3 - s_2) \log(s_1) \log(1-s_1-s_2),
\end{aligned}$$

$$\begin{aligned}
v_6 = {} & -96(1-s_1)^2(1-s_2)^2 s_2 (s_1^4 + 2 s_2 s_1^3 - 2 s_1^3 + s_2^2 s_1^2 - 4 s_2 s_1^2 + s_1^2 - 2 s_2^2 s_1 \\
& + 3 s_2 s_1 - 2 s_1 + s_2^2 + 1) \log(s_1) \log(s_1+s_2),
\end{aligned}$$

$$v_7 = 48(1-s_1)(s_2-1)^2 s_2 (1-s_1-s_2)(6 s_2 s_1^3 - 6 s_1^3 - 11 s_2 s_1^2 + 15 s_1^2 + 3 s_2 s_1 - 9 s_1 + 2) \log(1-s_1),$$

$$\begin{aligned}
v_8 = {} & 96(1-s_1)(s_2-1)^2 (s_2 s_1^5 - s_1^5 + 2 s_2^2 s_1^4 - 5 s_2 s_1^4 + 3 s_1^4 + s_2^3 s_1^3 - 5 s_2^2 s_1^3 + 8 s_2 s_1^3 - 2 s_1^3 \\
& - s_2^3 s_1^2 + 4 s_2^2 s_1^2 - 4 s_2 s_1^2 + s_1^2 - 4 s_2^2 s_1 + 3 s_2 s_1 - s_1 - s_2^2 + s_2) \log(1-s_1) \log(s_1+s_2),
\end{aligned}$$

$$\begin{aligned}
v_9 = {} & 48(1-s_1)(1-s_2)(s_2^2 s_1^5 - s_2 s_1^5 - 9 s_2^3 s_1^4 + 16 s_2^2 s_1^4 - 8 s_2 s_1^4 + s_1^4 - 9 s_2^4 s_1^3 + 46 s_2^3 s_1^3 - 67 s_2^2 s_1^3 \\
& + 35 s_2 s_1^3 - s_1^3 + s_2^5 s_1^2 + 16 s_2^4 s_1^2 - 67 s_2^3 s_1^2 + 84 s_2^2 s_1^2 - 43 s_2 s_1^2 + s_1^2 - s_2^5 s_1 - 8 s_2^4 s_1 + 35 s_2^3 s_1 \\
& - 43 s_2^2 s_1 + 22 s_2 s_1 - s_1 + s_2^4 - s_2^3 + s_2^2 - s_2) \log^2(s_1+s_2),
\end{aligned}$$

$$\begin{aligned}
v_{10} = {} & -96(1-s_1)(1-s_2)(1-s_1-s_2)(s_2^2 s_1^3 - s_2 s_1^3 + s_2^3 s_1^2 - 3 s_2^2 s_1^2 + 2 s_2 s_1^2 \\
& - s_1^2 - s_2^3 s_1 + 2 s_2^2 s_1 + s_2 s_1 - s_2^2) \log(1-s_1-s_2),
\end{aligned}$$

$$v_{11} = 24(1-s_1)(1-s_2)(1-s_1-s_2)(6s_2^3s_1^3 - 12s_2^2s_1^3 + 7s_2s_1^3 - s_1^3 - 12s_2^3s_1^2 + 24s_2^2s_1^2 - 14s_2s_1^2 + 7s_2^3s_1 - 14s_2^2s_1 + 12s_2s_1 - s_1 - s_2^3 - s_2)\log^2(1-s_1-s_2),$$

$$v_{12} = 96s_1(1-s_2)^2(1-s_1-s_2)(s_2s_1^4 - s_1^4 + s_2^2s_1^3 - 4s_2s_1^3 + 3s_1^3 - 5s_2^2s_1^2 + 8s_2s_1^2 - 2s_1^2 + 7s_2^2s_1 - 11s_2s_1 + s_1 - 2s_2^2 + 5s_2 - 1)\mathrm{Li}_2(s_1),$$

$$v_{13} = 96(1-s_1)(1-s_2)(1-s_1-s_2)(s_2^2s_1^4 - 2s_2s_1^4 + s_1^4 + 8s_2^3s_1^3 - 17s_2^2s_1^3 + 12s_2s_1^3 - 3s_1^3 + s_2^4s_1^2 - 17s_2^3s_1^2 + 32s_2^2s_1^2 - 20s_2s_1^2 - 2s_2^4s_1 + 12s_2^3s_1 - 20s_2^2s_1 + 20s_2s_1 - 2s_1 + s_2^4 - 3s_2^3 - 2s_2)\mathrm{Li}_2(1-s_1-s_2),$$

$$v_{14} = v_2(s_1 \leftrightarrow s_2), \quad v_{15} = v_3(s_1 \leftrightarrow s_2), \quad v_{16} = v_5(s_1 \leftrightarrow s_2), \quad v_{17} = v_6(s_1 \leftrightarrow s_2),$$
$$v_{18} = v_7(s_1 \leftrightarrow s_2), \quad v_{19} = v_8(s_1 \leftrightarrow s_2), \quad v_{20} = v_{12}(s_1 \leftrightarrow s_2).$$

APPENDIX B: RELEVANT PHASE-SPACE FORMULAS

1. Double differential phase-space for the 3-particle final state

The kinematical variables s_1 and s_2 are defined as

$$s_1 = \frac{(p_b - q_1)^2}{m_b^2}, \qquad s_2 = \frac{(p_b - q_2)^2}{m_b^2}, \tag{B1}$$

where p_b and q_i denote the four-momenta of the b quark and the photons, respectively. The kinematics of the process $b \to s\gamma\gamma$ is fully described by s_1 and s_2. The formula for the double differential decay width is therefore free of additional phase-space integration variables. It reads

$$\frac{d\Gamma_{1\to3}}{ds_1 ds_2} = \frac{1}{4}\frac{(4\pi)^{-3+2\epsilon}}{\Gamma[2-2\epsilon]} m_b^{1-4\epsilon} s_1^{-\epsilon} s_2^{-\epsilon} \times (1-s_1-s_2)^{-\epsilon}|M_3|^2. \tag{B2}$$

The variables s_1 and s_2 vary in the range

$$0 \le s_1 \le 1, \qquad 0 \le s_2 \le 1 - s_1.$$

2. Triple differential phase space for the 4-particle final state

The kinematical variables s_1, s_2, and s_3 are defined as

$$s_1 = \frac{(p_b - q_1)^2}{m_b^2}, \qquad s_2 = \frac{(p_b - q_2)^2}{m_b^2}, \qquad s_3 = \frac{(p_s + k)^2}{m_b^2}, \tag{B3}$$

where p_b, p_s, k, and q_i denote the four-momenta of the b quark, the s quark, the gluon, and the photons, respectively. The kinematics is fully described in terms of five phase-space variables x_1, x_2, x_3, x_4, and x_5 as given explicitly in Eqs. (3.6), (3.9), and (3.10) in Ref. [42]. By identifying k_1, k_2, k_3, and k_4 given there with the four-momenta of the two photons, the s quark and the gluon, respectively, we easily derive from the information in [42] the formula for the triple differential decay width. We remind the reader that in this paper we consider only the range in s_1 and s_2 with

$$0 \le s_1 \le 1, \qquad 0 \le s_2 \le 1 - s_1,$$

which is also accessible to the three-body decay $b \to s\gamma\gamma$. For this case we obtain

$$\frac{d\Gamma_{1\to4}}{ds_1 ds_2 ds_3} = \frac{(4\pi)^{-6+3\epsilon}2^{-4\epsilon}\Gamma[1-\epsilon]}{(1-2\epsilon)\Gamma^2[1-2\epsilon]} m_b^{3-6\epsilon} s_3^{-\epsilon} \times (s_1s_2 - s_3)^{-\epsilon}(1 - s_1 - s_2 + s_3)^{-\epsilon} \times \int dx_4 dx_5 [x_4(1-x_4)]^{-\epsilon}[x_5(1-x_5)]^{-1/2-\epsilon}|M_4|^2, \tag{B4}$$

where x_1, x_2, and x_3 (appearing in $|M_4|^2$) are understood to be expressed in terms of s_1, s_2, and s_3 according to

$$x_1 = s_1, \qquad x_2 = \frac{s_3}{s_1}, \qquad x_3 = \frac{s_1s_2 - s_3}{(1-s_1)(s_1 - s_3)}. \tag{B5}$$

x_4 and x_5 vary between zero and 1, while $s_3 \in [0, s_1s_2]$.

APPENDIX C: RENORMALIZATION CONSTANTS

In this Appendix, we collect the explicit expressions of the renormalization constants needed for the ultraviolet renormalization in our calculation (see Sec. III).

The operator $\mathcal{O}_7$, as well as the b-quark mass contained in this operator, is renormalized in the $\overline{\mathrm{MS}}$ scheme [43]:

$$Z_{77}^{\overline{\mathrm{MS}}} = 1 + \frac{4C_F}{\epsilon}\frac{\alpha_s(\mu)}{4\pi} + O(\alpha_s^2),$$
$$Z_{m_b}^{\overline{\mathrm{MS}}} = 1 - \frac{3C_F}{\epsilon}\frac{\alpha_s(\mu)}{4\pi} + O(\alpha_s^2). \quad \text{(C1)}$$

All the remaining fields and parameters are renormalized in the on-shell scheme. The on-shell renormalization constant for the b-quark mass is given by

$$Z_{m_b}^{\mathrm{OS}} = 1 - C_F\Gamma(\epsilon)e^{\gamma\epsilon}\frac{3-2\epsilon}{1-2\epsilon}\left(\frac{\mu}{m_b}\right)^{2\epsilon}\frac{\alpha_s(\mu)}{4\pi} + O(\alpha_s^2), \quad \text{(C2)}$$

while the renormalization constants for the s- and b-quark fields are

$$Z_{2s}^{\mathrm{OS}} = 1 + O(\alpha_s^2),$$
$$Z_{2b}^{\mathrm{OS}} = 1 - C_F\Gamma(\epsilon)e^{\gamma\epsilon}\frac{3-2\epsilon}{1-2\epsilon}\left(\frac{\mu}{m_b}\right)^{2\epsilon}\frac{\alpha_s(\mu)}{4\pi} + O(\alpha_s^2). \quad \text{(C3)}$$

The various quantities δZ appearing in Sec. III are defined to be $\delta Z = Z - 1$.

[1] M. Misiak *et al.*, Phys. Rev. Lett. **98**, 022002 (2007).
[2] T. Hurth and M. Nakao, Annu. Rev. Nucl. Part. Sci. **60**, 645 (2010).
[3] A. J. Buras, arXiv:1102.5650.
[4] H. Simma and D. Wyler, Nucl. Phys. **B344**, 283 (1990).
[5] L. Reina, G. Ricciardi, and A. Soni, Phys. Lett. B **396**, 231 (1997).
[6] L. Reina, G. Ricciardi, and A. Soni, Phys. Rev. D **56**, 5805 (1997).
[7] J. J. Cao, Z. J. Xiao, and G. R. Lu, Phys. Rev. D **64**, 014012 (2001).
[8] K. G. Chetyrkin, M. Misiak, and M. Munz, Phys. Lett. B **400**, 206 (1997); **425**, 414(E) (1998).
[9] K. Melnikov and A. Mitov, Phys. Lett. B **620**, 69 (2005).
[10] H. M. Asatrian, T. Ewerth, A. Ferroglia, P. Gambino, and C. Greub, Nucl. Phys. **B762**, 212 (2007).
[11] A. Kapustin, Z. Lint, and H. D. Politzer, Phys. Lett. B **357**, 653 (1995).
[12] A. Gemintern, S. Bar-Shalom, and G. Eilam, Phys. Rev. D **70**, 035008 (2004).
[13] C.-H. V. Chang, G.-L. Lin, and Y.-P. Yao, Phys. Lett. B **415**, 395 (1997).
[14] G. Hiller and E. O. Iltan, Phys. Lett. B **409**, 425 (1997).
[15] S. W. Bosch and G. Buchalla, J. High Energy Phys. 08 (2002) 054.
[16] S. W. Bosch, arXiv:hep-ph/0208203.
[17] G. Hiller and A. S. Safir, J. High Energy Phys. 02 (2005) 011.
[18] G. Hiller and A. S. Safir, Proc. Sci., HEP2005 (2006) 277.
[19] G. L. Lin, J. Liu, and Y. P. Yao, Phys. Rev. Lett. **64**, 1498 (1990).
[20] S. Herrlich and J. Kalinowski, Nucl. Phys. **B381**, 501 (1992).
[21] S. R. Choudhury, G. C. Joshi, N. Mahajan, and B. H. J. McKellar, Phys. Rev. D **67**, 074016 (2003).
[22] T. M. Aliev, G. Hiller, and E. O. Iltan, Nucl. Phys. **B515**, 321 (1998).
[23] S. Bertolini and J. Matias, Phys. Rev. D **57**, 4197 (1998).
[24] I. I. Bigi, G. Chiladze, G. Devidze, C. Hanhart, A. Liparteliani, and U.-G. Meissner, arXiv:hep-ph/0603160.
[25] G. G. Devidze and G. R. Jibuti, arXiv:hep-ph/9810345.
[26] T. M. Aliev and G. Turan, Phys. Rev. D **48**, 1176 (1993).
[27] Z. J. Xiao, C. D. Lu, and W. J. Huo, Phys. Rev. D **67**, 094021 (2003).
[28] Q. XiuMei, W. Huo, and X. Yang, Chinese Phys. C **33**, 252 (2009).
[29] W. J. Huo, C. D. Lu, and Z. J. Xiao, arXiv:hep-ph/0302177.
[30] H. Chen and W. Huo, arXiv:1101.4660.
[31] A. Y. Ignatiev, G. C. Joshi, and B. H. J. McKellar, Int. J. Mod. Phys. A **20**, 4079 (2005).
[32] C. Anastasiou, L. J. Dixon, and K. Melnikov, Nucl. Phys. B, Proc. Suppl. **116**, 193 (2003).
[33] C. Anastasiou and K. Melnikov, Nucl. Phys. **B646**, 220 (2002).
[34] C. Anastasiou, L. J. Dixon, K. Melnikov, and F. Petriello, Phys. Rev. D **69**, 094008 (2004).
[35] S. Laporta, Int. J. Mod. Phys. A **15**, 5087 (2000).
[36] F. V. Tkachov, Phys. Lett. **100B**, 65 (1981).
[37] K. G. Chetyrkin and F. V. Tkachov, Nucl. Phys. **B192**, 159 (1981).
[38] C. Anastasiou and A. Lazopoulos, J. High Energy Phys. 07 (2004) 046.
[39] A. V. Smirnov, J. High Energy Phys. 10 (2008) 107.
[40] E. Remiddi, Nuovo Cimento Soc. Ital. Fis. A **110**, 1435 (1997).
[41] M. Argeri and P. Mastrolia, Int. J. Mod. Phys. A **22**, 4375 (2007).
[42] H. M. Asatrian, A. Hovhannisyan, V. Poghosyan, T. Ewerth, C. Greub, and T. Hurth, Nucl. Phys. **B749**, 325 (2006).
[43] M. Misiak and M. Munz, Phys. Lett. B **344**, 308 (1995).